

Wolframin Expression Induces Novel Ion Channel Activity in Endoplasmic Reticulum Membranes and Increases Intracellular Calcium*

Received for publication, September 17, 2003
Published, JBC Papers in Press, October 3, 2003, DOI 10.1074/jbc.M310331200

Abdullah A. Osman‡, Mitsuyoshi Saito‡, Carol Makepeace‡, M. Alan Permutt§, Paul Schlesinger‡¶, and Mike Mueckler‡

From the ‡Department of Cell Biology and Physiology and §Department of Medicine, Washington University School of Medicine, St. Louis, Missouri 63110

Wolfram syndrome is an autosomal recessive neurodegenerative disorder associated with juvenile onset non-autoimmune diabetes mellitus and progressive optic atrophy. The disease has been attributed to mutations in the WFS1 gene, which codes for a protein predicted to possess 9–10 transmembrane segments. Little is known concerning the function of the WFS1 protein (wolframin). Endoglycosidase H digestion, immunocytochemistry, and subcellular fractionation studies all indicated that wolframin is localized to the endoplasmic reticulum in rat brain hippocampus and rat pancreatic islet β -cells, and after ectopic expression in *Xenopus* oocytes. Reconstitution of wolframin from oocyte membranes into planar lipid bilayers demonstrated that the protein induced a large cation-selective ion channel that was blocked by Mg^{2+} or Ca^{2+} . Inositol triphosphate was capable of activating channels in the fused bilayers that were similar to channel components induced by wolframin expression. Expression of wolframin also increased cytosolic calcium levels in oocytes. Wolframin thus appears to be important in the regulation of intracellular Ca^{2+} homeostasis. Disruption of this function may place cells at risk to suffer inappropriate death decisions, thus accounting for the progressive β -cell loss and neuronal degeneration associated with the disease.

Wolfram syndrome, or diabetes insipidus, diabetes mellitus, optic atrophy disorder (DIDMOAD),¹ is an autosomal recessive disease, suggesting a loss of function (1, 2). Wolfram patients demonstrate non-inflammatory atrophic changes in the brain (3) and in pancreatic islets, resulting in progressive diabetes, blindness, deafness, and other severe neurological defects (4). Genetic analysis has demonstrated that mutations in the WFS1 gene are clearly associated with the DIDMOAD syndrome (2, 5). The Wolfram gene encodes a 100-kDa tetrameric

protein (wolframin) possessing 9–10 predicted transmembrane segments (6). However, no clear sequence similarities have been identified that might shed light on the function of the protein (7). Northern blot analysis has revealed prominent expression of wolframin mRNA in affected tissues, including the brain and pancreas (1, 7). These expression sites correlate well with the atrophic changes associated with the syndrome.

It was suggested that wolframin may be a mitochondrial protein (8), because many of the clinical features characteristic of this syndrome are similar to defects in oxidative phosphorylation that are seen in mitochondrial diseases, such as MELAS (mitochondrial encephalomyopathy, lactic acidosis, and stroke-like symptoms), Leber's hereditary optic neuropathy, and maternally inherited diabetes and deafness (mitochondrial diabetes). Supporting this hypothesis, deletions of mitochondrial DNA have been reported in some Wolfram patients (9). However, recent reports have provided direct evidence to refute this hypothesis (10, 11). Various homozygous or compound heterozygous mutations, including nonsense, frameshift, deletion, insertion, and missense mutations were identified in Wolfram patients without revealing a clear relation between these mutations and phenotype (12). Although Wolfram syndrome is rare, heterozygous carriers have been reported as 26 times more likely to require hospitalization for depression and psychiatric illness, leading to the hypothesis that heterozygosity for WFS1 gene mutations may be a significant cause of psychiatric illness in the general population (13). An increased prevalence of diabetes mellitus in first degree relatives of Wolfram patients has also been reported (14). Recently, several single amino acid mutations associated with Wolfram's disease have been associated with type 2 diabetes in non-Wolfram patients (2, 5).

A recent report has shown that wolframin is localized to the ER when overexpressed in cultured fibroblasts (11). This localization suggests that wolframin may play an as yet undefined role in membrane trafficking, secretion, processing, and/or regulation of ER calcium homeostasis. Rapid but controlled redistribution of intracellular calcium is central in signaling, secretion, and apoptosis in all eukaryotic cells (15–22). The unfolded protein response and calcium regulation are well defined ER functions that have been shown to play prominent roles in cellular apoptosis (23–25). Calcium release and uptake by the ER are fundamental to calcium regulation but are thus far only partially understood (25).

Based on the pathophysiology of the syndrome, it appears reasonable that wolframin may be somehow involved in the survival pathways of pancreatic islet β -cells and neurons (26). The presence of 9–10 predicted transmembrane segments in wolframin suggested that it might function in the transport of

* This work was supported in part by National Institutes of Health Grants DK38495 (to M. M.), AR46539 (to P. S.), and DK16746 (to M. A. P.). The costs of publication of this article were defrayed in part by the payment of page charges. This article must therefore be hereby marked "advertisement" in accordance with 18 U.S.C. Section 1734 solely to indicate this fact.

¶ To whom correspondence and reprint requests should be addressed: Dept. of Cell Biology and Physiology, Washington University School of Medicine, 660 S. Euclid Ave., St. Louis, MO 63110. Tel.: 314-362-2223; Fax: 314-362-7463; E-mail: paul@cellbio.wustl.edu.

¹ The abbreviations used are: DIDMOAD, diabetes insipidus, diabetes mellitus, optic atrophy disorder; WFS1, Wolfram syndrome 1 gene or protein; IP₃, inositol 1,4,5-triphosphate; μ F, microfarad(s); pS, picosiemens(s); ER, endoplasmic reticulum; MBS, modified Barth's saline; TRPV, transient receptor potential vallerinoid-like; HEK, human embryonic kidney.

ions or other small molecules across membranes. In the present study, we conducted a series of experiments to test this hypothesis. Immunohistochemical studies of the rat pancreas confirmed that wolframin is primarily localized in the islet β -cells, present at low levels in α -cells and absent from the exocrine tissue. We demonstrate that ectopic expression of wolframin in *Xenopus* oocytes results in its strict localization to the endoplasmic reticulum, consistent with the subcellular localization of the native protein in mammalian cells. Expression of wolframin in oocytes produced an increase in cytosolic Ca^{2+} and induced novel cation-selective channel activities in ER membranes. Given that Ca^{2+} regulation by the ER is prominent in cellular apoptosis, these data suggest that wolframin may be involved in the regulation of ER-mediated cellular mortality and that a defect in this regulatory process is the cause of the progressive β -cell loss and neuronal degeneration associated with the disease.

MATERIALS AND METHODS

Preparation of Anti-WFS1 Antiserum and Western Blot Analysis

Antibody directed against WFS1 was generated using a synthetic peptide corresponding to the 20 N-terminal amino acids of WFS1 coupled to keyhole limpet hemocyanin via an N-terminal cysteine residue. Immunization of rabbits and production of antiserum was conducted by Charles River Laboratories (Southbridge, MA) according to their standard protocols. IgG was purified from the rabbit antiserum using protein A-agarose. SDS-PAGE and immunoblotting were carried out after transfer of proteins to nitrocellulose membranes (MSI, Westborough, MA). ^{125}I -Labeled goat anti-rabbit or anti-mouse IgG (at 1:500 dilution, Amersham Biosciences) was used as the secondary antibody. Signals were visualized by autoradiography.

Expression of Human WFS1 in *Xenopus* Oocytes

Full-length human WFS1 cDNA was subcloned into the oocyte expression vector pSP64T. *Xenopus laevis* or *Xenopus tropicalis* oocytes were isolated and prepared for injection according to published methods (27). Briefly, stage V to VI oocytes were isolated from excised ovaries and treated with 2 mg/ml type II collagenase (Sigma) in modified Barth's saline (MBS) for 15 min at room temperature, washed extensively in MBS supplemented with 5% bovine serum albumin, and maintained in MBS plus bovine serum albumin at 18 °C for all subsequent procedures. After an overnight incubation, healthy oocytes lacking a vitellin layer were selected using a dissecting microscope. WFS1 mRNA was prepared from BglII-linearized pSP64T. *In vitro* transcription was performed using SP6 RNA polymerase system (Promega). Oocytes were injected with 50 nl of water (sham) or 50 ng of cRNA and then incubated for 3 days at 18 °C before analysis.

Glycosylation Analysis

N-Glycanase Digestion—Thirty μg of intracellular membranes purified from oocytes and 50 μg of rat brain hippocampal tissue lysate were solubilized in 1% SDS, adjusted to a final concentration of 0.25% SDS, 1.9% Nonidet P-40, 30 mM Tris-HCl, pH 8.0, 25 mM 2-mercaptoethanol, and then digested with 0.25 units of N-glycanase (Enzyme, Boston, MA) overnight at 37 °C.

Endoglycosidase H Digestion—*Xenopus* oocyte intracellular membranes and rat brain hippocampal tissue lysate were digested with endoglycosidase H overnight at 37 °C in a 25- μl total reaction volume containing 0.5 liters of 3 M sodium acetate, pH 5.5, and 0.3 milliunits of enzyme (Roche Molecular Biochemicals). All membranes were analyzed by SDS-PAGE followed by immunoblotting as described above.

Confocal Immunofluorescence Microscopy and Immunohistochemistry

Frozen thin sections of oocyte were prepared as described previously (27), and HEK293 cells were obtained from American Type Culture Collection (ATCC). Thin sections and cell monolayers were analyzed by laser confocal immunofluorescence microscopy using protein A-agarose-purified anti-WFS1 antibody (1:100 dilution) and fluorescein-conjugated goat anti-rabbit IgG (1:500 dilution) (Cappel, Durham, NC). Rat pancreas sections were prepared, and immunohistochemical analysis was performed as described previously (28) with some modifications. Briefly, rats were killed by decapitation and pancreata were removed. Pancreata were fixed in 10% formalin and embedded in paraffin for

serial sectioning (5 μm thickness). Antigen unmasking was performed by treating the tissue sections in 10 mM sodium citrate buffer, pH 6.0, at 95 °C for 5 min. Tissue sections were incubated with anti-WFS1 and mouse anti-BiP (Santa Cruz Biotechnology, Santa Cruz, CA) antibodies at 1:50 dilution for 1 h at room temperature in phosphate-buffered saline containing 2% goat serum, then with secondary antibodies (Alexa 594 goat anti-rabbit IgG, Alexa 488 goat anti-mouse IgG) (1:500 dilution; Molecular Probes). For detection of WFS1 in pancreatic islets, sections were processed by a modification of the indirect immunoperoxidase method (29), using mouse anti-insulin and anti-glucagon primary antibodies (1:500, Sigma) and the anti-WFS1 antibody followed by incubation with the secondary antibody as described. Fluorescence was detected using a Bio-Rad MRC-600 laser scanning confocal microscope.

Measurements of Intracellular Calcium in Oocytes

X. tropicalis oocytes were placed in a tissue chamber on the stage of an inverted fluorescence microscope (Axiovert 100M, Zeiss, Lambda 10-Z, Sutter Instrument Co.). Free cytosolic calcium was determined by incubating *Xenopus* oocytes with fura-2 AM (Molecular Probes) for 30 min at room temperature. Each oocyte was then exposed to 340 and 380 nm excitation wavelengths, respectively. The filter control and data acquisition were carried out using Slidebook, version 3.0.4.9 (Intelligent Imaging Innovations, Cambridge, MA). The excitation light passed through a 10 \times objective lens to the oocyte through a dichroic mirror. All experiments were carried out at room temperature. Ca^{2+} concentrations were determined by converting the 340 nm/380 nm fura-2 fluorescence ratios to free $[\text{Ca}^{2+}]$ using *in situ* calibration with Ca^{2+} -EGTA standards (Molecular Probes, Eugene, OR).

Preparation of Oocyte Microsomal Membranes

X. laevis oocytes were injected with cRNA from either wild-type or mutant (I269S, R456H) WFS cDNA, and ER membranes were prepared as described previously (30) with some modifications. Briefly, after collagenase treatment, oocytes were rinsed five times with 5 volumes of H/K buffer (90 mM KCl, 50 mM HEPES, pH 7.1). Stage V–VI oocytes were selected, and the volume of packed oocytes was measured. All residual H/K buffer was removed, and a volume of ice-cold sucrose/H/K (40% sucrose weight/volume in H/K buffer containing 3 mM MgCl_2) equal to the volume of the oocytes was added. All subsequent steps were performed at 4 °C. The oocytes were gently broken open by passing the mixture through a 3.8-cm 19-gauge needle 10 times. The homogenate was centrifuged for 3 min at 3000 $\times g$. The cloudy gray supernatant was then gently mixed and transferred to a fresh centrifuge tube, and the pellet was discarded. This process was repeated three times. The resulting milky white supernatant was mixed gently and diluted with 0.3 volume of cold H/K buffer. The microsomal membranes were pelleted by centrifugation at 10,000 $\times g$ for 10 min. The supernatant was discarded and the membranes were resuspended in H/K buffer containing 3 mM MgCl_2 and then either used directly for SDS-PAGE or stored at -80 °C for bilayer experiments.

Reconstitution of Microsomal Membranes from Oocytes into Planar Lipid Bilayers and Channel Activity Measurements

Planar lipid bilayers were prepared from azolectin type II (Sigma) according to published methods (31). The lipids, 70% dioleoylphosphatidylcholine and 30% dioleoylphosphatidic acid, were dissolved in decane at 30 mg/ml and stored under nitrogen until use. Briefly, 2 μl of lipid solution was applied to 0.25-mm orifice of a polystyrene cuvette (Warner Instruments, Hamden, CT), and the solvent was allowed to evaporate. The cuvette was then placed into a bilayer chamber and connected to a bilayer clamp (BC525-c; Warner Instruments) by Ag/AgCl electrodes via agar bridges. Data were collected using CLAMPEX 8.0 (Axon Instruments, Foster City, CA), archived on videotape using a Neurocorder DR-484 (Neuro Data Instruments, Delaware Water Gap, PA), and analyzed using ORIGIN (Microcal, Amherst, MA) and CLAMPFIT (Axon Instruments). Bilayers were formed by spreading with a polished glass rod and allowed to thin to a capacitance of 0.4 $\mu\text{F}/\text{cm}^2$, at which point the noise was typically 0.2 pA and the leak conductance was 20 pS. The salt concentrations were initially 150 mM KCl in the cis and trans chamber and adjusted to a 450 mM in the cis chamber as indicated. Outward (positive) currents were defined as K^+ moving cis to trans. All solutions were buffered to pH 7.0 with 10 mM K-HEPES. Oocyte microsomal membranes (10 μg of protein) were added to the cis chamber with mixing. To vary calcium concentration in the bilayer, EGTA and CaCl_2 were added. The MilliQ water employed for buffers in these studies averaged 30 μM Ca^{2+} . When low calcium was required, 300 μM EGTA was added to the buffer, reducing the free

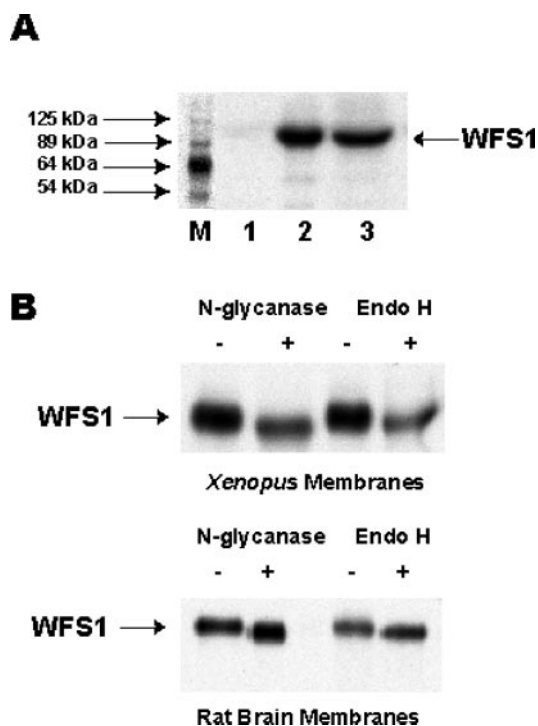


FIG. 1. Detection of native and ectopically expressed wolfram in rat hippocampus and *Xenopus* oocytes and sensitivity of wolfram to glycosidase digestion. A, total membrane lysates (50 μ g of protein) from oocytes and hippocampal tissues obtained from rat brain were subjected to SDS-PAGE (7.5% acrylamide gel) and Western blot analysis was performed using anti-WFS1 antibody. The positions of molecular size markers (M) are indicated on the left. Anti-WFS1 antibody detected a 100-kDa band in the total membrane lysate of oocytes injected with WFS1 cRNA (lane 2) prepared as described under "Materials and Methods." Lane 1 represents oocytes injected with water (sham) as control. Anti-WFS1 antibody recognized endogenous WFS1 protein in hippocampal homogenate (lane 3). B, digestion of total membrane lysates obtained from oocytes injected with WFS1 cRNA (upper panel) or rat brain hippocampus (lower panel) with either N-glycanase or endoglycosidase H (Endo H) followed by immunoblot analysis. The WFS1 immunoreactive band was completely sensitive to digestion by both N-glycanase and endoglycosidase H.

calcium to less than 1 μ M. High calcium was obtained by adding 100 μ M CaCl_2 to the buffer.

Animal Experiments

All experimental protocols were approved by the Animal Studies Committee and conducted according to the Guidelines for Animal Research at Washington University School of Medicine.

RESULTS

Generation and Characterization of Wolfram Antibody—Rabbits were immunized with a synthetic peptide corresponding to the 20 N-terminal amino acids of human wolfram. Characterization of the wolfram antiserum was conducted by immunoblot analysis using membranes from *Xenopus* oocytes injected with wolfram mRNA. The anti-wolfram antibody detected a distinct band migrating at a molecular mass of ~100 kDa (Fig. 1A, lane 2). The observed band is consistent with the expected molecular mass of 100.29 kDa predicted from the hWFS1 cDNA. Specificity was confirmed by pre-incubation of the antibody with the wolfram immunizing peptide, which completely blocked the appearance of the 100-kDa band on the film (data not shown). The antibody also detected endogenous wolfram expressed in rat hippocampal tissue lysate (Fig. 2A, lane 3).

Wolfram Is Localized Exclusively to the Endoplasmic Reticulum Membrane—Previously published data suggested that wolfram is localized to endoplasmic reticulum (ER) mem-

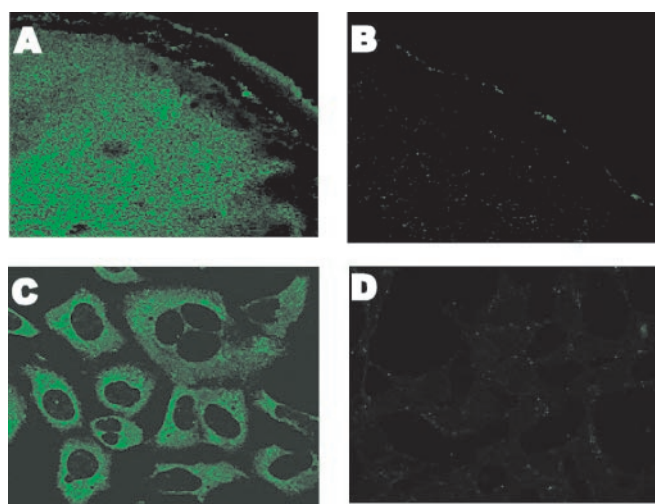


FIG. 2. Immunocytochemical localization of wolfram by laser confocal microscopy. Frozen thin sections were prepared from oocytes injected with WFS1 cRNA (A) or water (B) and then stained with WFS1 antibody as described under "Materials and Methods." HEK293 cells were stained with WFS1 antibody in the absence (C) or presence (D) of a 100-fold molar excess of immunizing peptide.

branes when overexpressed in primary human fibroblasts (12). To confirm these data for endogenous wolfram and determine the subcellular distribution of wolfram after ectopic expression, total membranes from *Xenopus* oocytes (Fig. 1B, upper panel) and rat brain hippocampus (Fig. 1B, lower panel) were prepared. Digestion of these membranes with N-glycanase, an enzyme that cleaves N-linked oligosaccharides from proteins, or endoglycosidase H, an enzyme that cleaves only high mannose core oligosaccharides from glycosylated proteins, was conducted. Western blot analysis showed a shift in the electrophoretic mobility of wolfram after digestion with either glycosidase (Fig. 1B). These data indicate that the N-linked oligosaccharides of wolfram, in both native cells and after ectopic expression of the protein in oocytes, are not processed to a complex form. This result strongly suggests that wolfram is strictly confined to the endoplasmic reticulum membrane.

The intracellular localization of endogenous and ectopically expressed wolfram was confirmed by indirect immunofluorescence microscopic analysis of frozen sections of *Xenopus* oocytes injected with wolfram cRNA, HEK293 cells, and rat pancreas. In oocytes, wolfram exhibited a granular cytoplasmic distribution, suggesting intracellular membrane labeling (Fig. 2A). Endogenous wolfram in HEK293 cells also demonstrated a granular cytoplasmic pattern, consistent with localization to intracellular membranes (Fig. 2C). Preadsorption of the WFS1 antibody with the immunizing peptide abolished labeling of pancreatic islet cells (Fig. 3, A–C). Interestingly, the β -cells of rat pancreatic islets stained strongly positive for wolfram (Fig. 3, D–F) and only slight staining was observed in the glucagon positive α -cells (Fig. 3, G–I). Double-labeling indirect immunofluorescence analysis using antibodies to wolfram and the ER marker, BiP, was consistent with the strict localization of wolfram to the ER (Fig. 3, J–L). These data confirm that wolfram is expressed predominantly, if not exclusively, in the endoplasmic reticulum in both native cell types and after ectopic expression in *Xenopus* oocytes.

Expression of Wolfram Induces Specific Ion Channel Activity in Planar Bilayers Derived from Endoplasmic Reticulum Membranes of *Xenopus* Oocytes—The presence of predicted transmembrane segments, a very mild similarity to the pore region of the transient receptor potential (TRP)-caspase channel family, and the lack of any other significant homology with

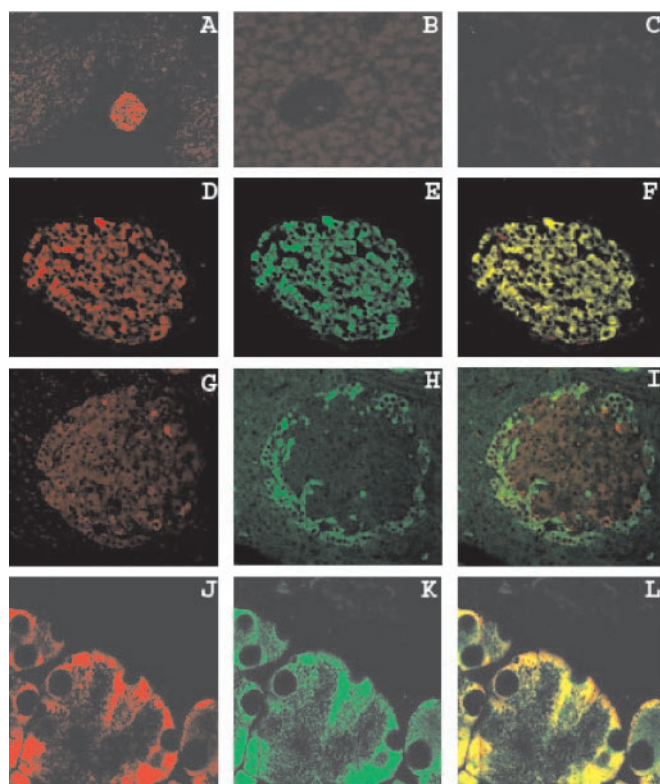


FIG. 3. Co-localization of wolframin and the ER marker BiP in rat pancreatic islet β -cells. Pancreata were prepared and stained with anti-WFS1 (Alexa 594, red), and anti-BiP (Alexa 488, green) antibodies for co-localization of WFS1, or with anti-insulin and anti-glucagon antibodies to compare the distribution of these proteins in pancreatic islets as described under "Materials and Methods." In all pancreata studied, the β -cells stained strongly positive for WFS1 (D and E). Very little staining was observed in glucagon secreting α -cells (G–I). D and G are wolframin labeled in red; insulin (E) and glucagon (H) are labeled in green. Overlapping red and green labeling appears in yellow (F and I). The staining of wolframin was blocked by pre-incubation of the antibody with 100-fold molar excess of immunizing peptide (B). Panel C represents a control experiment conducted in the absence of WFS1 antibody. Colocalization of the red WFS1 signal (J) and the green BiP (ER marker) signal (K) is indicated by the yellow signal (L).

a functional amino acid sequence suggested wolframin might be a novel cation channel in the ER membrane. Because of the strict localization of wolframin to the ER, it was necessary to use reconstitution into planar lipid bilayers to determine whether wolframin possessed channel activity. Microsomal membranes from control (sham-injected) and wolframin-expressing oocytes were studied in planar lipid bilayers using KCl salt solutions to determine how channel activity and its voltage dependence were affected by wolframin expression. The control membranes from four preparations, five preparations from wolframin-expressing oocytes, and two preparations expressing the mutant wolframin proteins were fused into bilayers a minimum of three times each, giving results that were qualitatively consistent. The magnitude of the currents from a fusion varied 5-fold, but several characteristics were reproducibly associated with wolframin expression and distinct from control membranes isolated from sham-injected oocytes. Single-channel records can be difficult to attain from isolated membrane fragments, and therefore the voltage dependence was determined from the mean current normalized to the mean current at zero applied potential in a KCl gradient, which allowed comparison between membrane preparations and individual fusions into bilayers.

A short segment representing the currents observed in control membranes is shown in Fig. 4. We employed all points

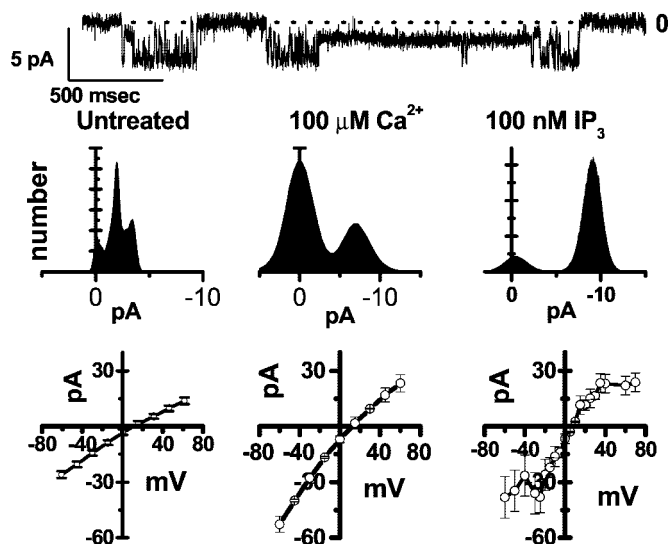
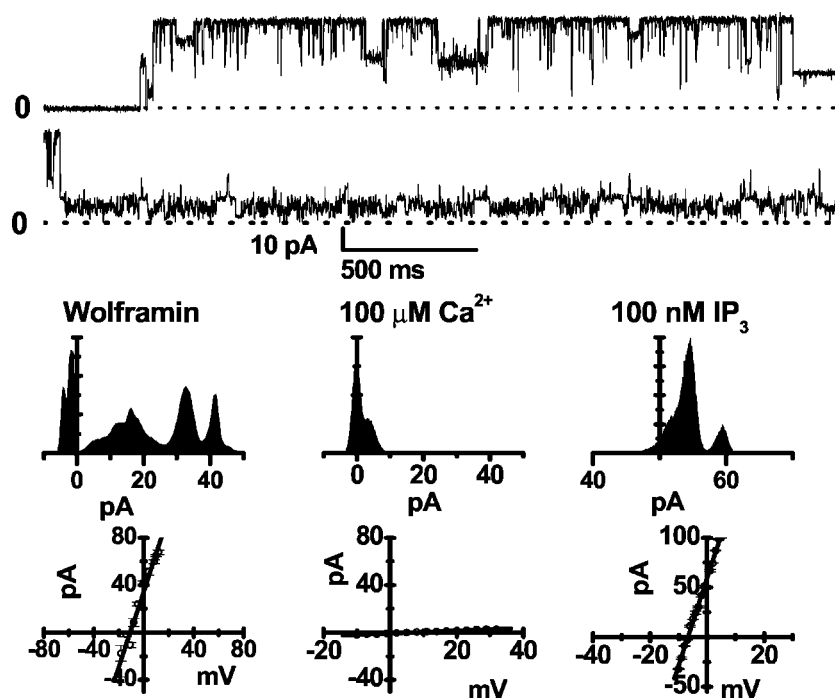


FIG. 4. Channel activity of microsomal membranes from control oocytes. Microsomal membranes isolated from water-injected control oocytes were allowed to fuse with $0.4 \mu\text{F}/\text{cm}^2$ bilayers in a 450/150 mM KCl gradient. The upper panel is a 3-s record from a typical recording of this preparation. This preparation was characterized by the all points currents histogram in the *Untreated* column. This histogram was obtained from 20 min of recording on four membrane preparations. The histograms for $100 \mu\text{M Ca}^{2+}$ and 100nM IP_3 columns represent 3–4 min of recording from two preparations of membranes. The voltage dependence values of these currents were obtained by averaging the current for 1 min at each applied potential. The slope conductance and reversal potential for each were determined by linear regression as follows: untreated, $326 \pm 10 \text{ pS}$ and 14.8 mV ; $100 \mu\text{M Ca}^{2+}$, $631 \pm 28 \text{ pS}$ and 16.3 mV ; or 100nM IP_3 , $1200 \pm 59 \text{ pS}$ and 6.5 mV . Each voltage dependence was studied in four membranes so that for the averages n is 4 or greater.

histograms to characterize the multichannel recordings that were observed in the reconstituted bilayers. An extensive summation of data from four membrane preparations yielding 2–8 min each of recording in a 450/150 mM KCl gradient is shown under the "untreated" heading. Under this trace is the voltage dependence summarized as an average from eight control bilayers. This series demonstrates that our membrane preparation contains a number of channels and that the normalization process allows the incorporation of data from separate experiments. In a KCl gradient, the control microsomes are dominated by inward currents representing chloride movement across the bilayer. We used the voltage dependence of these currents to study calcium and IP_3 effects on these membrane preparations. When $100 \mu\text{M Ca}^{2+}$ was added to bilayers containing control membranes, the histogram indicated one open state with a conductance approximately double that of control membranes in the absence of Ca^{2+} (Fig. 4, $100 \mu\text{M Ca}^{2+}$). The addition of 100nM IP_3 also increased the bilayer currents, but with a small decrease in reversal potential (Fig. 4, 100nM IP_3). These observations are consistent with previous studies on endoplasmic reticulum but do not exclude some contamination by other membrane components (32–35).

When microsomal membranes from oocytes expressing wolframin were studied in a 450/150 KCl gradient, strikingly different patterns were observed. Although the inward current patterns previously described were present in all membrane preparations, outward currents not seen in the controls were observed (Fig. 5). Wolframin-expressing membranes frequently displayed a conductance 5-fold larger than the examples shown here, but they were unstable and difficult to analyze. The histogram under the *Wolframin* heading in Fig. 5 is a summation of 20 min of recording in 10 membranes that had moderate to low conductance after fusion with membranes from wol-

FIG. 5. Channel activity of microsomal membranes from wolframin-expressing oocytes. Microsomal membranes isolated from wolframin injected oocytes were allowed to fuse with $0.4 \mu\text{F}/\text{cm}^2$ bilayers in a 450/150 mM KCl gradient. The upper panel is a 3-s record typical of the low conductance wolframin preparations. This preparation was characterized by the all points currents histogram in the *Wolframin* column. This histogram was obtained from 20 min of recording on 10 membrane preparations. The histograms for $100 \mu\text{M Ca}^{2+}$ and 100 nM IP_3 columns represent 3–4 min of recording from two preparations of membranes. The voltage dependence of these currents were obtained by averaging the current for 100 ms at each applied potential. The slope conductance and reversal potential for each were determined by linear regression as follows: wolframin, $3.19 \pm 0.19 \text{ nS}$ and -10.1 mV ; $100 \mu\text{M Ca}^{2+}$, $0.116 \pm 2.8 \text{ nS}$ and -5.92 mV ; 100 nM IP_3 , $8.78 \pm 0.015 \text{ nS}$ and -6.8 mV . Each voltage dependence is the average of at least four determinations.



fram-in-expressing oocytes. Routinely we saw multiple conductance levels in the outward currents and could identify two distinct phases of wolframin-associated channel activity. The large outward currents with multiple current levels shown at the top of Fig. 5 were the most distinctive wolframin-associated channels. This would occasionally develop into a second pattern, as shown in the second trace in Fig. 5, of smaller but much more regular channels. In bilayers with wolframin-associated channel activity, the outward currents occasionally alternated with inward currents identical to those that were seen in the control membrane (Fig. 5, *Wolframin*) but the two activity patterns were always separated by a period when the membrane was inactive. When $100 \mu\text{M Ca}^{2+}$ was added, there was a dramatic reduction of the wolframin-associated outward currents. The normalized slope conductance decreased from $3.19 \pm 0.193 \text{ nS}$ to $0.116 \pm 0.002 \text{ nS}$ ($n > 3$). Frequently the original currents were restored by the addition of EGTA to reduce total calcium to $<1 \mu\text{M}$. Typically, treatment with $100 \mu\text{M Ca}^{2+}$ did not directly produce the control membrane inward currents; however, periods of channel activity identical to those in Fig. 4 were observed. When 100 nM IP_3 was added to membranes while the wolframin-associated channels were active, there was a uniform increase in conductance that corresponded to $8.78 \pm 0.14 \text{ nS}$ ($n = 3$) for the example shown. This was accompanied by a shift in E_r to -6.77 mV , which is qualitatively similar to the increase in net outward current that was observed in membranes from sham-injected oocytes. Puromycin or signal peptides at $200 \mu\text{M}$ and adenophostin A had no effect upon the wolframin-associated channel activity (36, 37). The addition of $100 \mu\text{M Ca}^{2+}$ dramatically reduced the wolframin-associated outward currents in planar lipid bilayers (Fig. 6). In many trials the reduction in the normalized slope conductance was 90% or greater. Calcium also uniformly shifted the reversal potential in a 450/150 KCl gradient to the left (Fig. 6A). These effects were partially reversed by $500 \mu\text{M EGTA}$, which increased the currents but did not return the reversal potential to that seen in control membranes (Fig. 4). Divalent cation block of monovalent cation currents has previously been described to include both Ca^{2+} and Mg^{2+} in cells (38). Traditionally Mg^{2+} is included in buffers used in the isolation of intracellular membranes. In the presence of 2 mM

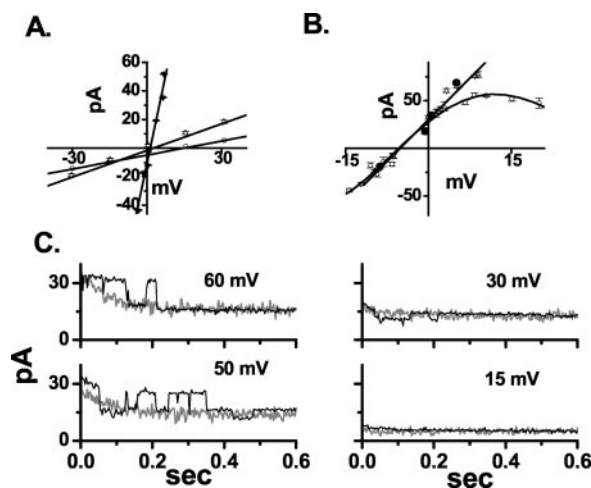


FIG. 6. Ca^{2+} and Mg^{2+} effects on wolframin-dependent ion channel activity in oocyte membranes. A, voltage dependence of the WFS1-associated currents. \circ , control ER; \triangle , WFS1 ER in $100 \mu\text{M CaCl}_2$; ∇ , ER after the addition of $500 \mu\text{M EGTA}$. B, data collected in a 450/150 KCl gradient (cis/trans) with $1 \mu\text{M Ca}^{2+}$ and 2 mM MgCl_2 (\circ), $300 \mu\text{M EGTA}$ and no MgCl_2 (\triangle), or instantaneous currents (10–25 ms) in 2 mM MgCl_2 (\bullet). C, four panels showing the time course of Mg^{2+} inactivation of wolframin-associated channels at several voltages (60, 45, 30, and 15 mV). The lighter trace results from the averaging of 5–10 sets of individual traces. This summation generates the equivalent of a macroscopic inactivation time series by averaging a group of records that show single-channel transitions. Panels A–C were collected in 450/150 KCl gradients with 2 mM MgCl_2 added as indicated. Data in A and B were normalized as described under “Materials and Methods” to allow comparison of data from different membranes. The data in C were not normalized.

Mg^{2+} , the wolframin-associated currents showed a mild voltage-dependent rectification that disappeared upon removal of the Mg^{2+} (Fig. 6B). This rectification was time-dependent, and instantaneous currents showed no sign of the rectification (Fig. 6B). In some preparations it was possible to observe a voltage-dependent effect of Mg^{2+} directly. This appeared as a rapid reduction of open channels upon application of positive potentials. By averaging multiple records for each voltage level, it was possible to generate a time course approximating a mac-

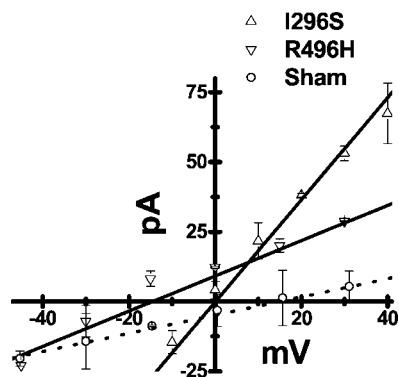


FIG. 7. Channel activity of microsomal membranes from oocytes expressing mutant wolframin proteins. Microsomal membranes isolated from wolframin mutant (I296S or R456H) cRNA-injected oocytes were allowed to fuse with $0.4 \mu\text{F}/\text{cm}^2$ bilayers in a 450/150 mM KCl gradient. Three successful fusions to planar lipid bilayers were studied for each mutant R456H (Δ) or I196S (\circ). The mean normalized voltage response and S.D. are plotted with linear fitting yielding for I296S a slope conductance of 1.83 ± 0.05 nS and $E_r = 1 \pm 0.3$ mV, and for R456H a slope conductance of 632 ± 46 pS and $E_r = -14.6 \pm 1.8$ mV. The addition of $100 \mu\text{M}$ CaCl_2 produced no significant changes in the voltage dependence of these currents.

roscopic inactivation time course for the Mg^{2+} effect and to clearly demonstrate the voltage dependence. A consistent characteristic of the wolframin-associated channel activity was this susceptibility to inhibition by the divalent cations Mg^{2+} and Ca^{2+} . In the next section we show that this was lost in a wolframin point mutant.

Several mutations in the WFS1 gene have been associated with Wolfram syndrome (39–41). The existence of these mutations provides a means of testing the possible physiological relevance of the observed cation channel activity induced by wolframin in oocyte membranes. If the observed oocyte channel activity is relevant to the physiological function of wolframin, we would predict that this activity should be altered by mutations associated with the disease. One mutant protein containing an amino acid substitution within a putative transmembrane domain of wolframin (R456H) and a second mutant protein containing an amino acid substitution within the soluble N-terminal region of wolframin (I296S) were studied in planar lipid bilayers. The mutant cRNAs produced proteins of the expected molecular weight after injection into *Xenopus* oocytes (data not shown). The channel activity observed in oocyte membranes expressing the mutants was distinct from that observed for wild-type wolframin-expressing oocytes or control oocytes. The mutant proteins induced voltage-dependent currents with the E_r shifted to 0.040 ± 0.008 mV for I296S and -14.5 ± 2.8 mV for R456H (see Fig. 7). Distinct from wild-type wolframin, where $100 \mu\text{M}$ Ca^{2+} reduced the cation selective currents by 90% (Fig. 6A), the membranes expressing the I296S mutant proteins showed no detectable inhibition by the addition of $100 \mu\text{M}$ Ca^{2+} (data not shown).

Effect of Wolframin Expression on Intracellular Calcium Levels—These studies indicate that either wolframin is a novel ER cation channel or, alternatively, regulates ER channel activities. Because ER cation channels are involved in regulating cytosolic calcium levels in response to various stimuli (42), the effect of wolframin expression on intracellular calcium levels was measured in oocytes. Fig. 8 illustrates the effect of wolframin expression on cytosolic free calcium concentrations in *X. tropicalis* oocytes. Fura-2 staining revealed that the $[\text{Ca}^{2+}]_i$ of wild-type wolframin-expressing oocytes was 646 ± 185 nM ($n = 18$), a value significantly greater ($p = 0.05$) than the values observed in sham-injected oocytes (155 ± 50 nM, $n = 26$), Glut1-expressing oocytes (140 ± 60 nM, $n = 14$) or oocytes

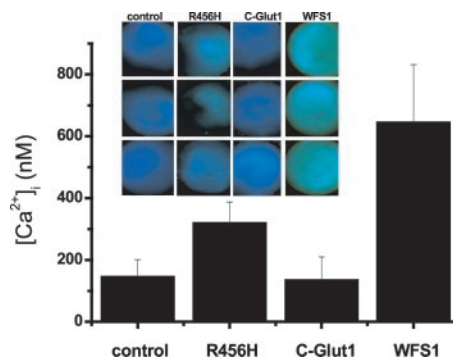


FIG. 8. Intracellular calcium in wolframin-expressing cells. Expression of WFS1 protein increases free cytosolic calcium levels in *Xenopus* oocytes. Intracellular calcium levels in oocytes expressing C-Glut1, controls, mutant R456H, or WFS1 were measured by loading oocytes with fura-2-AM as described under “Materials and Methods.” Fluorescence was monitored with an inverted fluorescence microscope assisted with a computer-driven program system. These results represent the means \pm S.E. of experiments in which the operator did not know which experimental groups individual oocytes belonged to until after the compilation of the results. Each experimental group included 10–20 oocytes, and the experiments were repeated four times. C-Glut1 cRNA and water-injected oocytes served as controls. Statistical analysis was conducted using analysis of variance, which indicated that only the wolframin group was significantly different ($p = 0.05$) from Glut-1, control, or the R456H mutant.

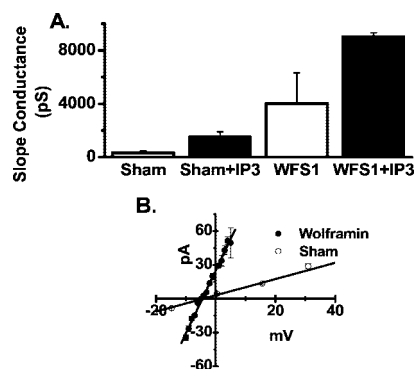


FIG. 9. IP_3 -induced cation channel activity in membranes from wolframin-expressing oocytes. A, summary and direct comparison of the effect of IP_3 on the slope conductance of microsomal membranes from sham-injected (*Sham*) and wolframin-expressing oocytes reconstituted into planer lipid bilayers. IP_3 was added to a final concentration of 100 nM where indicated. B, current-voltage plots of the IP_3 -dependent currents from control and wolframin-expressing microsomal membranes. Subtraction of basal channel activity used linear slope conductance determined from the voltage dependence of the untreated membranes that are shown in Figs. 4 and 5. After subtraction point-by-point of four IP_3 -treated membranes, the mean and S.D. were calculated. Linear least squares analysis of IP_3 -dependent currents indicated the slope conductance and reversal potential to be 720 ± 150 pS and -4.17 ± 0.82 mV for sham membranes and 5580 ± 145 pS and -4.46 ± 0.14 mV for wolframin membranes.

expressing the R456H wolframin mutant (325 ± 55 nM, $n = 16$) (Fig. 8). The Glut1-expressing oocytes served as a control for the possible nonspecific effects of ectopic membrane protein expression.

Effect of IP_3 on Channel Activity in Endoplasmic Reticulum Membranes from Wolframin-expressing Oocytes—The IP_3 increases the conductance of the endoplasmic reticulum and nuclear membranes to allow the release of Ca^{2+} for intracellular signaling (43). We observed that the application of 100 nM IP_3 to microsomal membranes from either sham or wolframin-expressing oocytes was followed by an increase of slope conductance and changes of reversal potential that reflect the activation of the IP_3 receptors in our membrane preparations (Figs. 4 and 5). In control membranes, IP_3 increased the mean

conductance from 326 to 1200 pS (Fig. 9A). Membranes overexpressing wolframin exhibited a conductance increase of 5590 pS (Fig. 9A). To compare the IP₃-dependent currents from sham and wolframin membranes, we used the normalized current-voltage relationships shown in Figs. 4 and 5 to subtract the basal currents from those observed at each voltage after IP₃ addition. The resulting voltage dependence of sham and wolframin membranes is shown in Fig. 9B. The reversal voltage is identical for both membranes, but the slope conductance is much larger in the membranes from oocytes expressing heterologous wolframin.

DISCUSSION

Wolfram syndrome is an autosomal recessive neurodegenerative disorder associated with juvenile onset non-autoimmune diabetes and progressive bilateral optic atrophy (1, 2). The WFS1 gene responsible for Wolfram syndrome was discovered by a positional cloning strategy (7). However, no clear sequence similarities have been identified in the public data bases that might shed light on the function of the protein. To gain insight into the function of the WFS1 protein, we studied its expression, processing, and localization in *Xenopus* oocytes, hippocampal tissue, and cultured cells using a polyclonal antibody directed against the N terminus of human wolframin. Our results indicate that wolframin is an endoglycosidase H-sensitive membrane glycoprotein confined to the ER in both native tissues and after ectopic expression in *Xenopus* oocytes. Additionally, our immunohistochemical studies on rat pancreas revealed a staining pattern for wolframin representative of β -cells of pancreatic islets. Because diabetes mellitus is recognized as a major clinical hallmark of Wolfram syndrome, these results suggest that the β -cell atrophy associated with this disease is likely to be a direct consequence of defective wolframin expression.

Membrane proteins located in the ER are often involved in protein processing, protein folding, or calcium homeostasis. Disrupting these processes can lead to cellular apoptosis (23, 44). It is possible that abnormal apoptosis is responsible for the non-inflammatory cellular degeneration that is observed in Wolfram syndrome (4). The amino acid sequence of wolframin lacks calcium or ATP binding motifs and contains no homology to heat shock proteins or GroEL, thereby providing no evidence for a direct involvement of wolframin in protein folding or calcium sequestration (45). Instead, our experimental evidence suggests that wolframin is associated with ion channel activity in the ER membrane. A distinguishing characteristic of the wolframin-dependent currents was sensitivity to Mg²⁺ and Ca²⁺ that was reduced in the Wolfram syndrome point mutants. Similar cation block in transient receptor potential valinoid-like (TRPV) channels results from channel occupancy at low concentrations of the divalent cations (46). Recently published gel filtration and cross-linking studies of wolframin in RIN and COS cells indicate that it exists as an oligomer, most likely a tetramer, in cellular membranes (6). Many voltage gated cation channels have been shown to be tetrameric (47). We were not able to show directly that the WFS1-dependent channels conducted Ca²⁺. However, overexpression of wild-type wolframin in oocytes increased cytosolic [Ca²⁺], consistent with increased release of calcium from the ER to the cytoplasm. Conversely, the point mutant forms of wolframin were not blocked by calcium and did not significantly increase cytosolic [Ca²⁺] when expressed in oocytes. These data suggest that wolframin may be a novel ER calcium channel with properties similar to the TRPV channels (48).

In addition, we determined that IP₃ application to sham membranes generated smaller slope conductance than it produced in membranes from wolframin-expressing cells. Because

the IP₃-dependent currents had the same reversal potential in both membranes, the larger voltage dependence we observed in membranes after heterologous wolframin expression suggests a possible increase of IP₃ receptors or enhanced sensitivity to IP₃.

Therefore, it remains possible that wolframin activates endogenous ER channels. Active secretory cells require rapid bi-directional ER calcium transfers to regulate cellular secretion and calcium homeostasis (49, 50). In mammalian cells the regulation of IP₃ receptor sensitivity is complex, showing both a biphasic response to Ca²⁺ and activation by ATP (51, 52). Recently, calcium sensor proteins that activate IP₃ receptor gating have been described (53). It is possible that wolframin activates a parallel pathway to IP₃-mediated Ca²⁺ release as well as functioning as a calcium-sensitive potassium channel that maintains ER membrane potential during calcium release.

In conclusion, the observations reported in this study suggest that wolframin may serve directly as a novel ER calcium channel or, alternatively, as a regulator of ER calcium channel activity. Interestingly, WFS1 mutations associated with Wolfram's disease reduced the susceptibility to cation block. It is possible that wolframin-mediated regulation of intracellular calcium provides an important protective function in secretory cells that are dependent on the ER for calcium signaling. Mutations that disrupt the calcium inhibition of this protein may stimulate cellular mortality decisions originating in the endoplasmic reticulum, thus leading to abnormal neuronal and β -cell degeneration that are characteristic of Wolfram syndrome.

Acknowledgments—We thank Drs. Alejandro Barbieri, Jim Huettner, Colin Nichols, and Fillepe Suarez for expert advice.

REFERENCES

- Raiti, S., Plotkin, S., and Newns, G. H. (1963) *Br. Med. J.* **2**, 1625–1629
- Hardy, C., Khanim, F., Torres, R., Scott-Brown, M., Seller, A., Poulton, J., Collier, D., Kirk, J., Polymeropoulos, M., Latif, F., and Barrett, T. (1999) *Am. J. Hum. Genet.* **65**, 1279–1290
- Rando, T. A., Horton, J. C., and Layzer, R. C. (1992) *Neurology* **42**, 1220–1224
- Karasik, A., O'Hara, C., Srikanta, S., Swift, M., Soeldner, J. S., Kahn, C. R., and Herskowitz, R. D. (1989) *Diabetes Care* **12**, 135–138
- Minton, J. A. L., Hattersley, A. T., Owen, K., McCarthy, M. I., Walker, M., Latif, F., Barrett, T., and Frayling, T. M. (2002) *Diabetes* **51**, 1287–1290
- Hoffmann, S., Philbrook, C., Gerbitz, K.-D., and Bauer, M. F. (2003) *Hum. Mol. Genet.* **12**, 2003–2012
- Inoue, H., Tanizawa, Y., Wasson, J. P. B., Kalidas, K., Bernal-Mizrachi, E., Mueckler, M., Marshall, H., Donis-Keller, H., Crock, P., Rogers, D., Mikuni, M., Kumashiro, H., Higashi, K., Sobue, G., Oka, Y., and Permutt, M. A. (1998) *Nat. Genet.* **20**, 143–148
- Bu, X., and Rotter, I. J. (1993) *Lancet* **342**, 598–600
- Barrientos, A., Casademont, J., Saiz, A., Cardellach, F., Volpini, V., Solans, A., Tolosa, E., Urbano-Marquez, A., Estivill, X., and Nunes, V. (1996) *Am. J. Hum. Genet.* **58**, 963–970
- Barrett, T. G., Scott-Brown, M., Seller, A., Bednarz, A., Poulton, K., and Poulton, J. (2000) *J. Med. Genet.* **37**, 463–466
- Takeda, K., Inoue, H., Tanizawa, Y., Matsuzaki, Y., Oba, J., Watanabe, Y., Shinoda, K., and Oka, Y. (2001) *Hum. Mol. Genet.* **10**, 477–484
- Awata, T., Inoue, K., Kurihara, S., Ohkubo, T., Inoue, I., Abe, T., Takino, H., Kanazawa, Y., and Katayama, S. (2000) *Biochem. Biophys. Res. Commun.* **268**, 612–616
- Swift, R. G., Polymeropoulos, M. H., Torres, R., and Swift, M. (1998) *Mol. Psychiatry* **3**, 86–91
- Polymeropoulos, M. H., Swift, R. G., and Swift, M. (1994) *Nat. Genet.* **8**, 95–97
- Granville, D. J., Ruehlmann, D. O., Choy, J. C., Cassidy, B. A., Hunt, D. W. C., van Breemen, C., and McManus, B. M. (2001) *Cell Calcium* **30**, 343–350
- Nakagawa, T., Zhu, H., Morishima, N., Li, E., Xu, J., Yankner, B. A., and Yuan, J. (2000) *Nature* **403**, 98–103
- Hajnoczky, G., Csordás, G., Madesh, M., and Pacher, P. (2000) *J. Physiol. (Lond.)* **529**, 69–81
- Szalai, G., Krischnamurthy, R., and Hajnoczky, G. (1999) *EMBO J.* **18**, 6349–6361
- He, H., Lam, M., McCormick, T. S., and Distelhorst, C. W. (1997) *J. Cell Biol.* **138**, 1219–1228
- Boya, P., Cohen, I., Zamzami, N., Vieira, H. L. A., and Kroemer, G. (2002) *Cell Death Differ.* **9**, 465–467
- Nutt, L. K., Pataer, A., Pahler, J., Fang, B., Roth, J., McConkey, D. J., and Swisher, S. G. (2002) *J. Biol. Chem.* **277**, 9219–9225
- Pan, Z., Bhat, M. B., Nieminen, A.-L., and Ma, J. (2001) *J. Biol. Chem.* **276**, 32257–32263
- Patil, C., and Walter, P. (2001) *Curr. Opin. Cell Biol.* **13**, 349–356
- Ferri, K. F., and Kroemer, G. (2001) *Nat. Cell Biol.* **3**, E255–E263
- Berridge, M. J., Lipp, P., and Bootman, M. D. (2000) *Nat. Rev. Mol. Cell Biol.*

- 1, 11–21
26. Gerbitz, K.-D. (1999) *Diabetologia* **42**, 627–630
27. Garcia, J. C., Strube, M., Leingang, K., Keller, K., and Mueckler, M. (1992) *J. Biol. Chem.* **267**, 7770–7776
28. Shinoda, K., Mon, S., Ohtsuki, T., and Osawa, Y. (1992) *J. Comp. Neuron* **322**, 360–376
29. Humason, G. L. (1997) *Animal Tissue Techniques*, pp. 361–378, The Johns Hopkins University Press, Baltimore
30. Kobilka, B. K. (1990) *J. Biol. Chem.* **265**, 7610–7618
31. Schlesinger, P., Gross, A., Xin, X., Yamamoto, K., Saito, M., Waksman, G., and Korsmeyer, S. (1997) *Proc. Natl. Acad. Sci. U. S. A.* **94**, 11357–11362
32. Franco-Obrego, A., Wang, H., and Clapham, D. E. (2000) *Biophys. J.* **79**, 202–214
33. Edwards, J., Tulk, B., and Schlesinger, P. (1998) *J. Membr. Biol.* **163**, 119–127
34. Schlesinger, P., Blair, H., Teitelbaum, S., and Edwards, J. (1997) *J. Biol. Chem.* **272**, 18636–18643
35. Landry, D., Sullivan, M., S. Nicolaidis, Redhead, C., Edelman, A., Field, M., Al-Awqati, Q., and Edwards, J. (1993) *J. Biol. Chem.* **268**, 14948–14955
36. Simon, S., and Blobel, G. (1991) *Cell* **65**, 371–380
37. Beckmann, R., Bubeck, D., Grassucci, R., Penczek, P., Verschoor, A., Blobel, G., and Frank, J. (1997) *Science* **278**, 2123–2126
38. Nilius, B., Vennekens, R., Prenen, J., Hoenderop, J. G. J., Bindels, R. J. M., and Droogmans, G. (2000) *J. Physiol. (Lond.)* **527**, 239–248
39. Bepalova, I. N., Van Camp, G., Bom, S. J., Brown, D. J., Cryns, K., DeWan, A. T., Erson, A. E., Flothmann, K., Kunst, H. P., Kurnool, P., Sivakumaran, T. A., Cremers, C. W., Leal, S. M., Burmeister, M., and Lesperance, M. M. (2001) *Hum. Mol. Genet.* **10**, 2501–2508
40. Eller, P., Föger, B., Gander, R., Sauper, T., Lechleitner, M., Finkenstedt, G., and Patsch, J. R. (2001) *J. Med. Genet.* **38**, e37
41. Storm, H. K., T. M. and, Hofmann, S., Gekeler, F., Scharfe, C., Rabl, W., Gerbitz, K. D., and Metinger, T. (1998) *Hum. Mol. Genet.* **7**, 2021–2028
42. Hille, B. (2001) *Ionic Channels of Excitable Membranes*, 3rd Ed., pp. 269–306, Sinauer Associates Inc., Sunderland, MA
43. Clapham, D. (1995) *Cell* **80**, 259–268
44. Kaufman, R. J. (1999) *Genes Dev.* **13**, 1211–1233
45. Ma, Y., and Hendershot, L. M. (2001) *Cell* **107**, 827–830
46. Pollock, N. S., Kargacin, M. E., and Kargacin, G. J. (1998) *Biophys. J.* **75**, 1759–1766
47. Hille, B. (2001) *Ionic Channels of Excitable Membranes*, 3rd Ed., pp. 405–440, Sinauer Associates Inc., Sunderland, MA
48. Gunthorpe, M. J., Benham, C. D., Randall, A., and Davis, J. B. (2002) *Trends Pharmacol. Sci.* **23**, 183–191
49. Shuai, J. W., and Jung, P. (2002) *Phys. Rev. Lett.* **88**, 068102-1–068102-4
50. Baran, I. (2003) *Biophys. J.* **84**, 1470–1485
51. Moraru, I. I., Kaftan, E. J., Ehrlich, B. E., and Watras, J. (1999) *J. Gen. Physiol.* **113**, 837–849
52. Elliott, A. C. (2001) *Cell Calcium* **30**, 73–93
53. Yang, J., McBride, S., Mak, D. D., Vardi, N., Palczewski, K., Haeseleer, F., and Foskett, J. K. (2002) *Proc. Natl. Acad. Sci. U. S. A.* **99**, 7711–7716